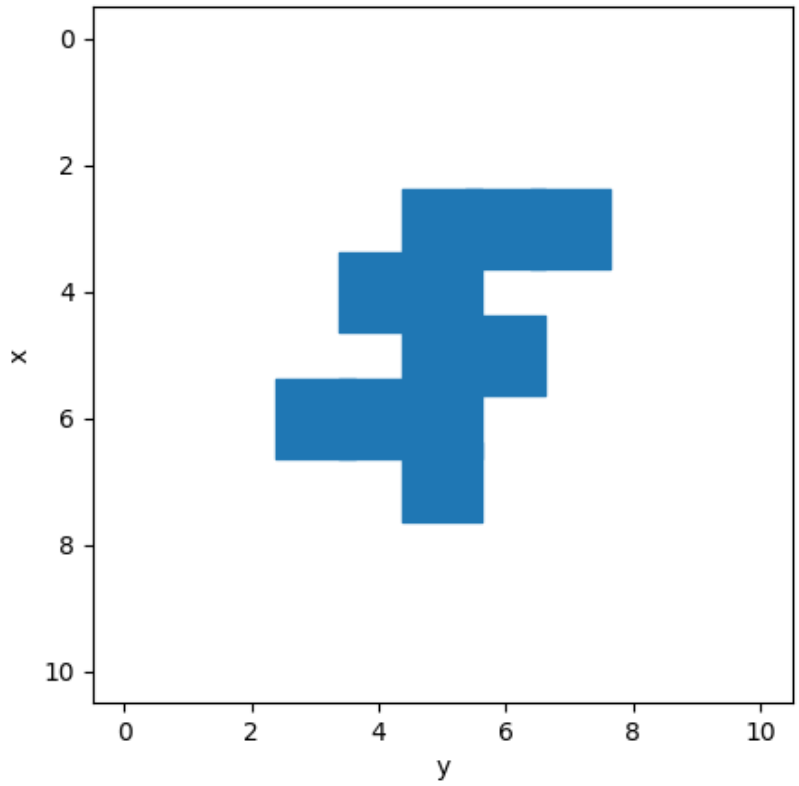

Figure 1. 2D diffusion limited aggregation (DLA) test case demonstrating the method used reproduces the expected behaviour. 10 particles were released one at a time from pre-determined spawn points along the 11×11 lattice and executed a random walk either moving up, down, left, or right at each step. If the walker left the lattice, it was bought back onto the opposite edge, imposing periodic boundaries. If the walker detected that at least one of its nearest-neighbour sites was occupied, it stuck. The random seed was set to '1234' so this procedure reproduced the characteristic F shape shown.

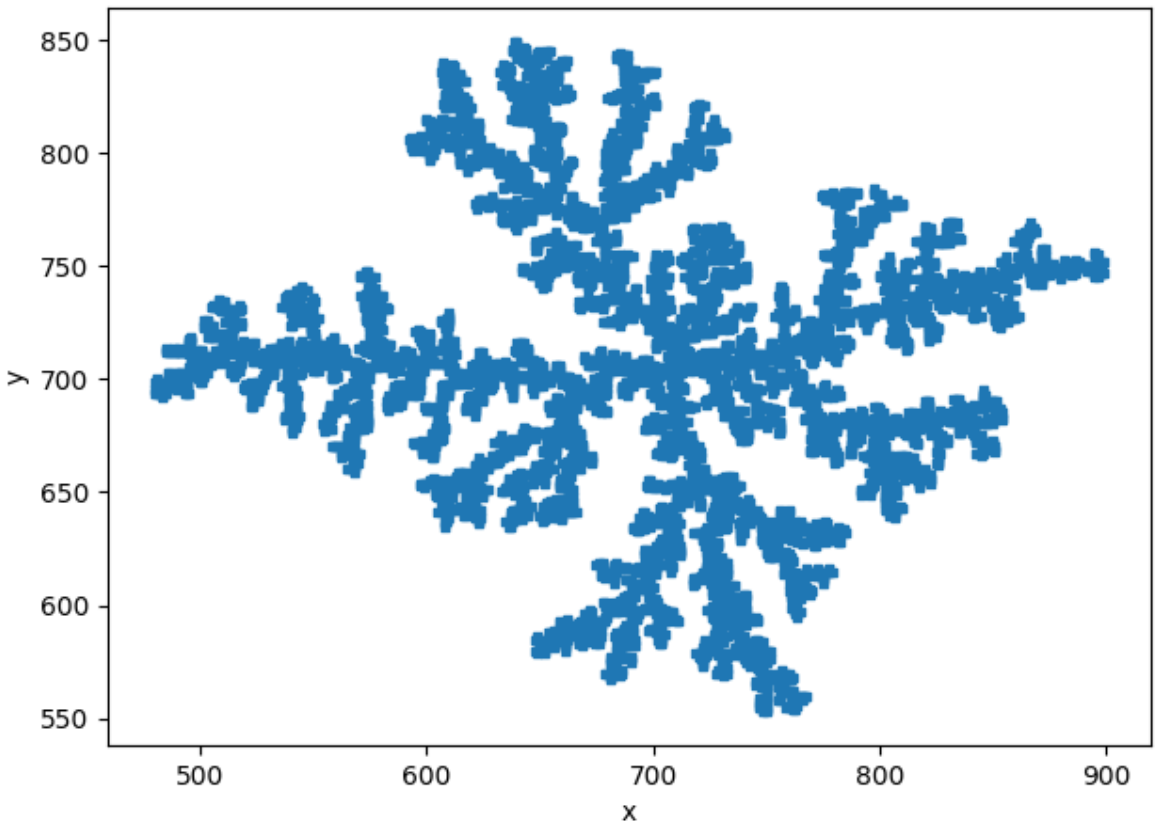

Figure 2. A scatter plot showing the 2D DLA cluster generated with 10,000 particles, a spawn-radius offset of 5, and a kill factor of 1.5. The spawn radius offset specifies how many lattice sites beyond the outermost occupied point the spawn circle is placed at each growth step. Walkers are introduced randomly on the circumference of this circle, which is centred on the seed particle, and undergo a lattice random walk until either attaching to the cluster or exceeding the kill radius. The total runtime of the simulation with these parameters was 13 minutes and 35 seconds. The resulting aggregate exhibits the characteristic branched cluster expected for 2D DLA. This figure demonstrates that the simulation produces physically reasonable cluster structures at larger scales.

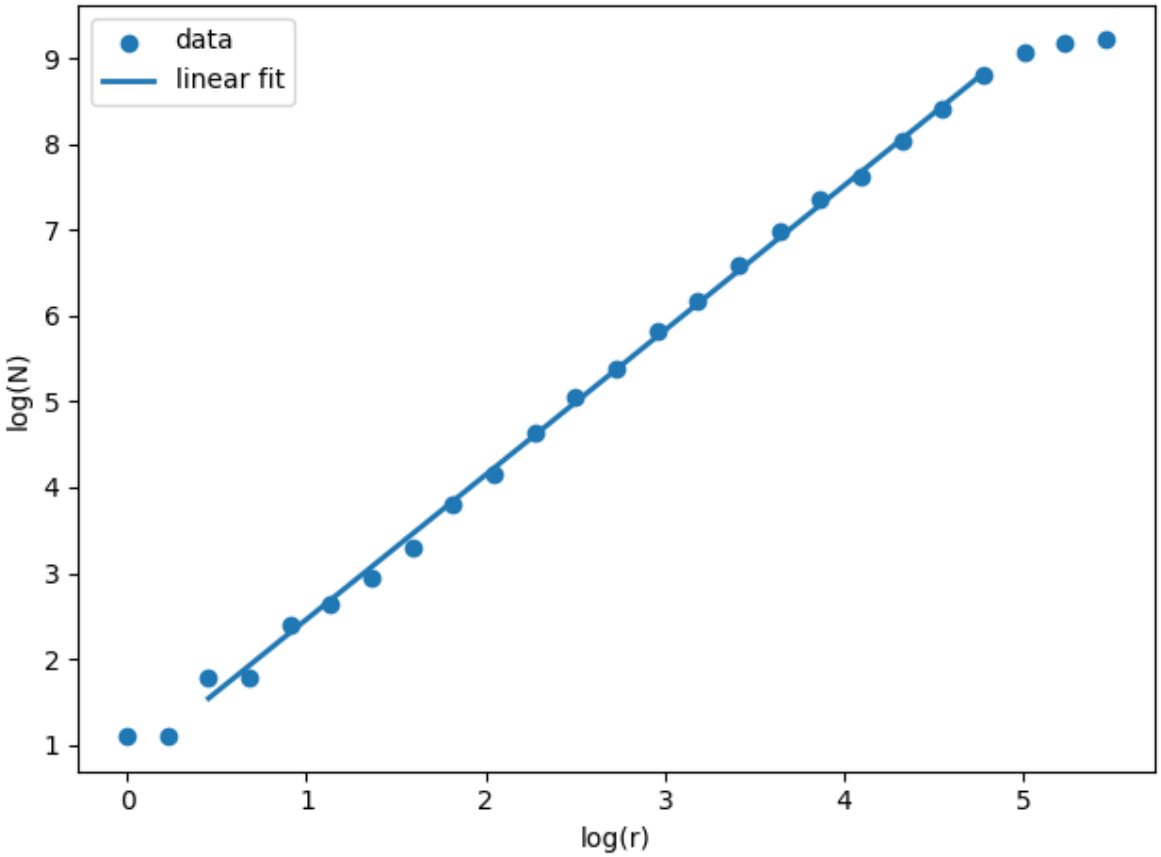

Figure 3. Log-log plot for the relationship between number of occupied sites, N, within a radius, r for the 2D DLA cluster shown in Figure 2. By taking the gradient of the linear section of this graph, shown by the blue line, the fractal dimension was determined to be $D = 1.685$, close to the expected value of $D \approx 1.7$. The spawn offset and the kill factor could both be increased to increase the accuracy of this. The number of particles and the lattice size could also be increased but would lead to a large increase in runtime for a comparatively smaller improvement in accuracy. The fractal dimension calculated provided quantitative validation that the model reproduces known theoretical results.

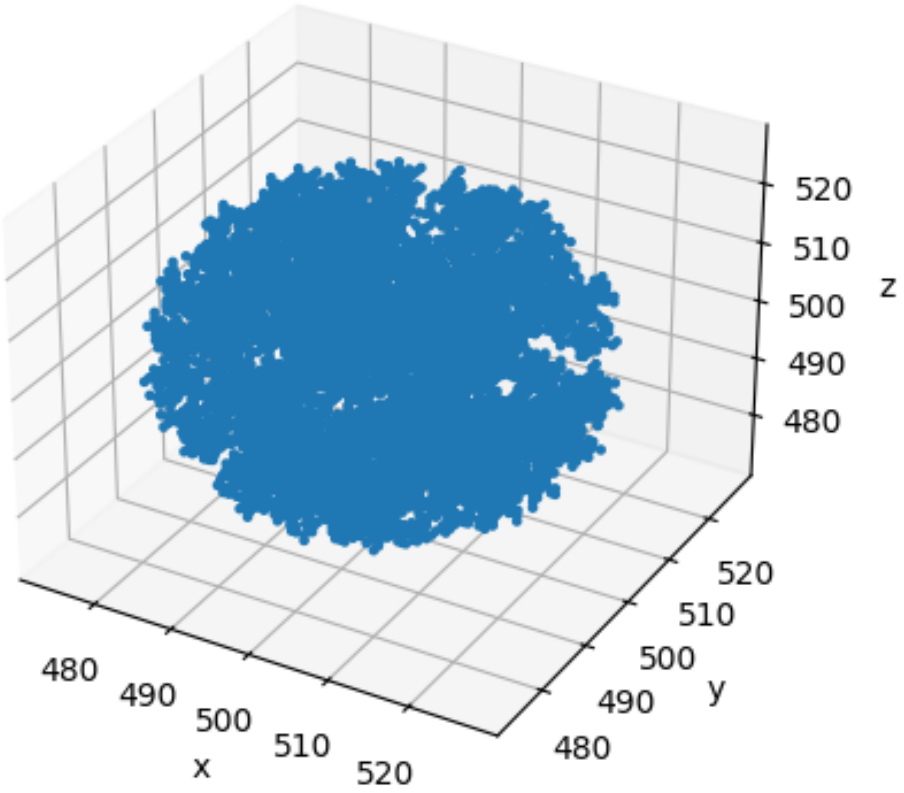

Figure 4. Scatter plot showing a 3D DLA cluster grown from 10,000 particles on a $1000 \times 1000 \times 1000$ lattice. Although the cluster branching is more difficult to see in the 3D plot due to overlapping branches, the fractal structure is still present. The spawn offset was 5, and the kill factor was set to 5 because 3D random walks escape more readily due to the additional degree of freedom; particles must therefore be introduced further from the cluster to avoid bias and maintain physically plausible growth. In 3D, recomputing the true cluster radius using np.where() at every particle attachment was very inefficient as it scans the entire lattice repeatedly. The 3D script therefore estimates the cluster radius scaling with cube root of particle number ($r \propto N^{1/3}$) and uses this estimate to set the spawn radius. This approximation is sufficient for this task and dramatically reduces runtime.

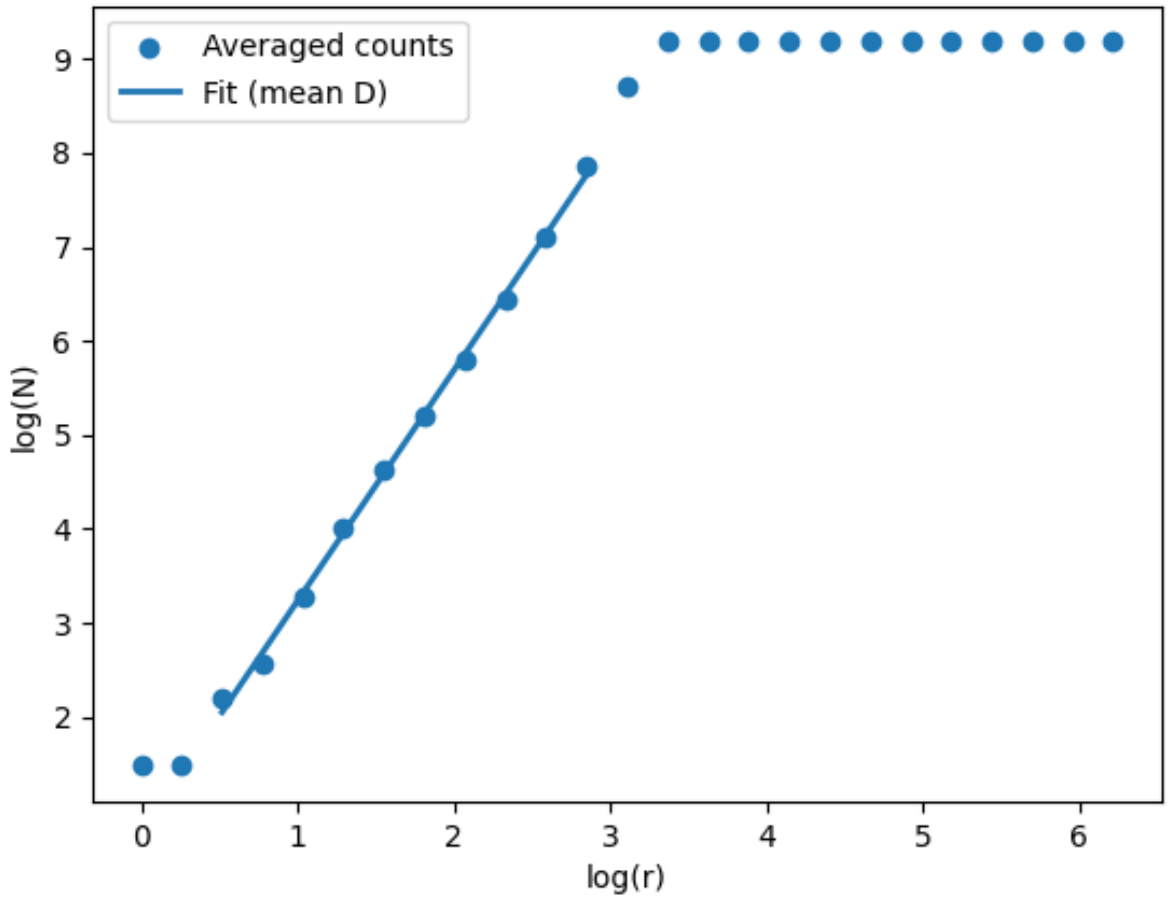

Figure 5. The $\log(N)$ vs $\log(r)$ plot for values of N and r averaged over 10 independent 3D DLA simulations of 10,000 particles each with the same parameters used to produce Figure 4. The linear fit, shown as the blue, has the gradient of the mean fractal dimension which was calculated to be $D = 2.45 \pm 0.05$. This agrees with the accepted theoretical range for 3D clusters of $D = 2.51 \pm 0.03$. This value demonstrates quantitatively that the 3D implementation of the algorithm also reproduces the expected results.

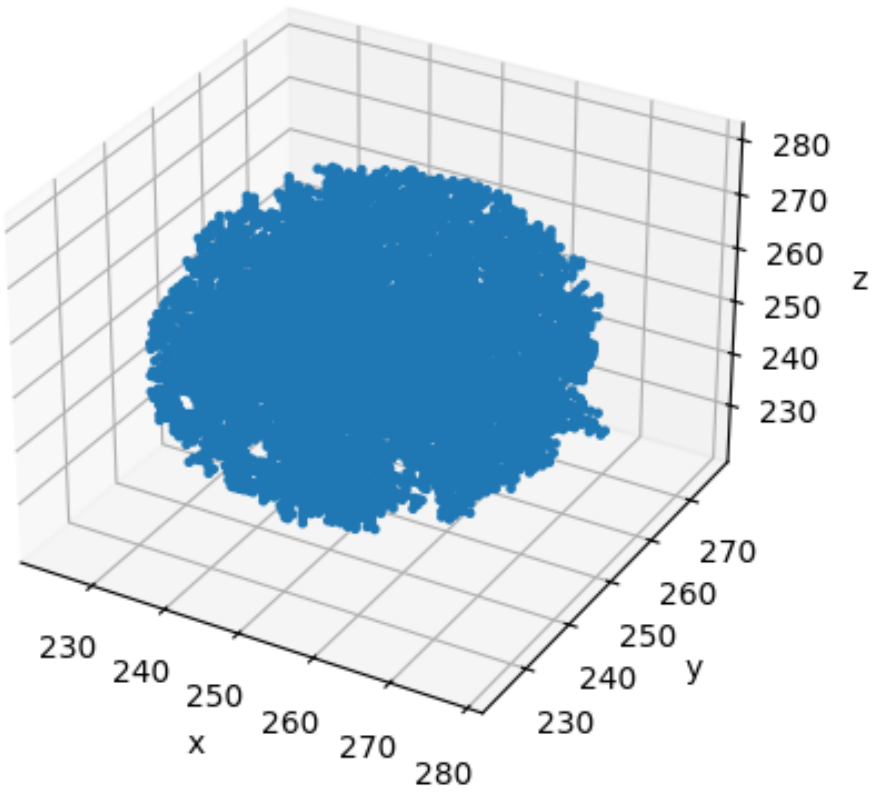

Figure 6. Scatter plot of a 3D DLA cluster grown from 10,000 particles on a $500 \times 500 \times 500$ lattice starting from an initial seed consisting of a one-dimensional line of 50 occupied sites, aligned parallel with the z axis. The smaller lattice was used to ensure the region where the effect of the seed was significant. The other starting parameters were all the same as the point particle. The line seed effectively lowered the dimension of the DLA growth when few particles were used. Whilst it is not possible to clearly see through the additional 3D growth, at low values of N, the growth of the cluster showed characteristics of a lower dimensional simulation. The central region of this cluster is denser than the central region of the cluster shown in Figure 4. Changing seed_type between point, line, and plane was used to investigate how initial geometry influences the measured fractal properties. The seed type primarily affects the scaling at small r (and small N), where the seed contributes a significant fraction of the occupied mass. As the cluster grows, the influence of the initial seed becomes less important, and the scaling approaches the bulk 3D DLA regime.

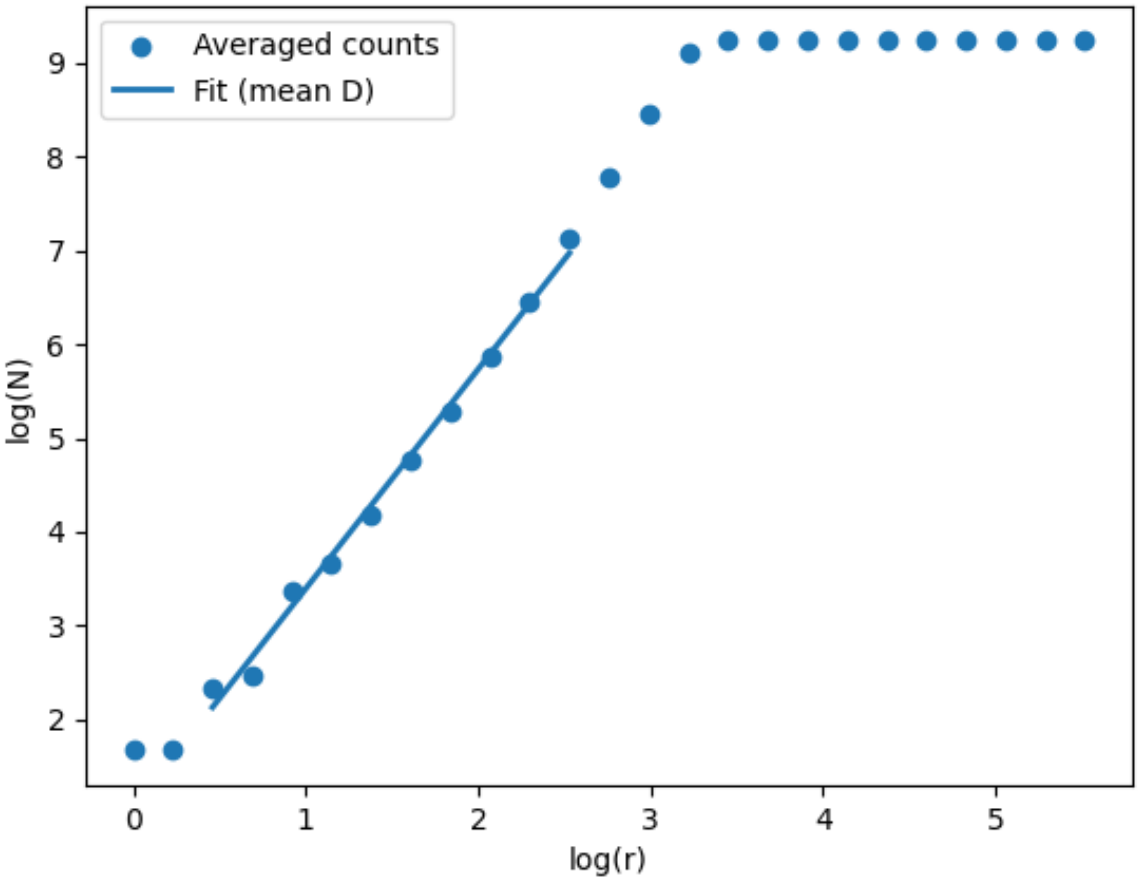

Figure 7. The mean $\log(N)$ vs $\log(r)$ plot for 10 simulations of the line-seed DLA cluster growth shown in Figure 6. At small radii the gradient is noticeably shallower than the point-seed case, reflecting that the growth is affected by the one-dimensional nature of the growth onto a line-seed. The mean fractal dimension of this region was calculated to be $D = 2.34 \pm 0.07$. This is expected for small N as the cluster can easily thicken around the line. As r increases, a distinct shoulder appears in the curve at $\log(r) \sim 1.7$ indicating a crossover towards purely three-dimensional branching once the cluster becomes large compared to the initial line length. Because the fractal dimension here is estimated using spherical counts N(r), the analysis is inherently spherical even when the seed geometry is not. This limits the physical conclusions that can be drawn about the differences between the three seeds. To investigate further, cylindrical counting could be used for the line seed for a better measure of the fractal properties at low r.

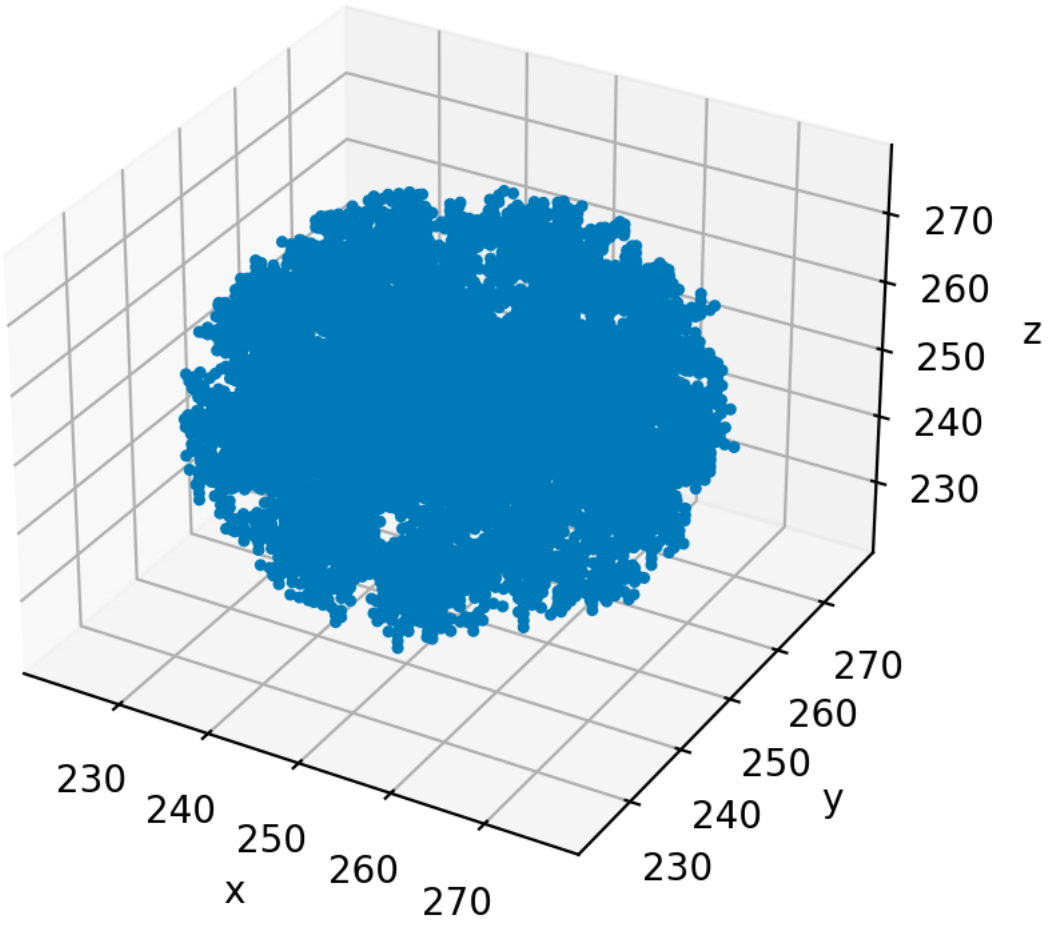

Figure 8. A scatter plot of a 3D DLA cluster grown from a plane seed consisting of a square of occupied sites in the x-y plane with length 50. Early growth thickens the plane before branching into the surrounding volume. At low N growth is mainly normal to the plane, leading to a fractal dimension characteristic of a lower dimensional simulation. As with the line seed a $500 \times 500 \times 500$ lattice was used. The density of the central region of this figure is clearly larger than in Figure 4.

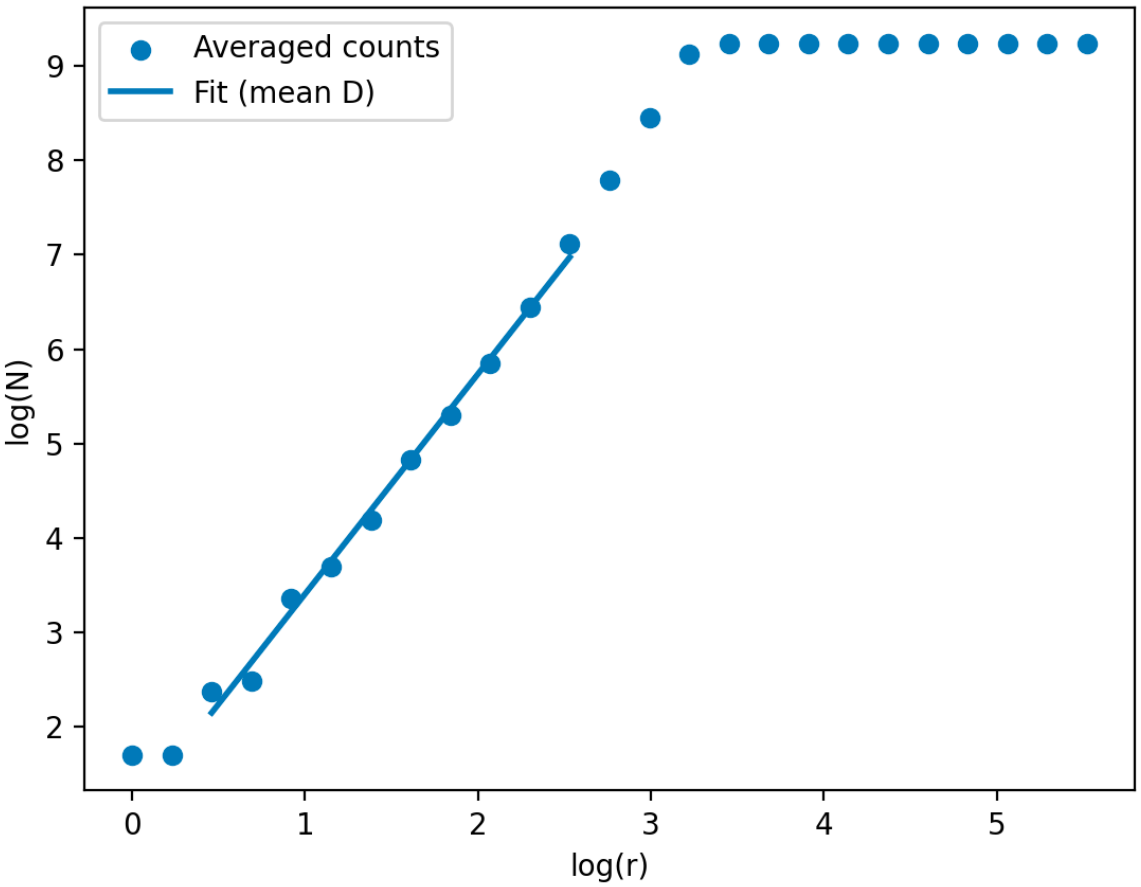

Figure 9. The $\log(N)$ vs $\log(r)$ plot averaged over 10 independent 3D diffusion limited aggregation simulations of 10,000 particles each. The mean fractal dimension of the small r section was calculated to be $D = 2.33 \pm 0.06$. Growth starts everywhere on the plane rather than around a point resulting in this lower fractal dimension compared to the point seed. The fractal dimensions obtained for line and plane seeds were found to be statistically indistinguishable. This indicates that, for the parameters chosen, both systems remain in a similar crossover region where the growth has not yet reached the asymptotic 3D DLA scaling. As with the line-seed case (Figure 7), the use of spherical counting limits the extent to which differences between seed geometries can be distinguished. The results of the experiment demonstrate that introducing lower dimensional seed geometries reduces the effective fractal dimension at small r because the seed dimension dominates the symmetry of the cluster. As the number of particles increases, the fractal dimension trends toward the standard 3D DLA value, consistent with the expectation that seed geometry primarily influences early growth and crossover behaviour rather than the large-scale DLA scaling.